GEOLOGIC PROSPECTING FOR MINERAL EXPLORATION IN THE TROODOS OPHIOLITE MASSIF OF CYPRUS USING LANDSAT TM DATA

Freek van der Meer
Lecturer in Geology
International Institute of Aerospace Surveys and Earth Sciences ITC
Department of Earth Resources Surveys, Geological Survey Division
350 Boulevard 1945
Enschede, the Netherlands

Commission VII, Working Group 4

KEY WORDS: Algorithms, Correlation, Geology, Resources, Classification, CCSM, Sulphide Mining, Cyprus

ABSTRACT

The island of Cyprus hosts one of the best preserved ophiolite (i.e. remnants of oceanic crust and mantle) sequences of the world: the Troodos massif. Lithologically the complex comprises a mantle series of ultramafic rocks overlain by gabbros and (plagio)granites. The crustal sequence consists of dyke swarms with two series of pillow lavas at the top known as the lower pillow lava and the upper pillow lava. Massive sulphide deposits, that have for long been the main income of Cyprus, occur at the contact between the lower and upper pillow lava series, however this contact is difficult to map in the field. In this paper we explore the possibility of using advanced image processing techniques to discriminate the main structural units to guide in mineral prospecting. A detailed field-spectral stratigraphic study forms the basis for the selection of potential spectral end-members characterizing the TM image used. A new image analysis techniques, Cross Correlogram Spectral Matching (CCSM), is introduced and succesfully applied to TM data from Cyprus.

INTRODUCTION

The Troodos massif of the island of Cyprus hosts one of the best preserved ophiolite (i.e. remnants of oceanic crust and mantle) sequences of the world. Massive sulphide deposits occur near the top of this sequence. The copper mining history of Cyprus dates back to Roman and Phoenician times (i.e. 3000 B.C.). Some 30 mines are located on the Troodos massif of which the largest deposit, the Mavrovouni mine, produced 15 million tons of ore averaging from 3.5 to 4.5% copper and 0.5% zinc. In the late 1970's all mines were closed due to the low copper prices. Only few studies have been conducted to explore the use of remote sensing for mineral exploration prospecting for sulphide deposits in this semi-arid environment (e.g. Davidson *et al.* 1993) although the Troodos massif forms an excellent test case since the geology has been studied in much detail and many deposits have been found. In this paper we explore the possibility of using remote sensing (using Landsat TM data) in combination with field spectroscopy to aid in mineral exploration. A new technique called Cross Correlation Spectral Matching will be introduced and applied.

GEOLOGY AND MINERAL DEPOSITS OF CYPRUS

The island of Cyprus (Fig. 1) is located in a tectonically active zone between the African lithospheric plate to the south and the Eurasian lithospheric plate to the north. Although many controversies still exists, most workers agree that Cyprus represents a slice of oceanic crust and mantle generated by rifting and subsequent up-thrusting initiated during the middle Cretaceous. Geologically Cyprus can be subdivided in four distinct geomorphological regions reflecting the changes in lithology: the Kyrenia range, the Mesaoria plain, the Troodos chain, and the Mamonia and circum-Troodos complex. This paper focuses on the ophiolite sequence exposed in the Troodos chain.

The Troodos mountain range is formed by a 10 to 20km thick ophiolite sequence of altered ultrabasic and basic plutonic igneous rocks capped by intermediate and basic lava flows. This ophiolite

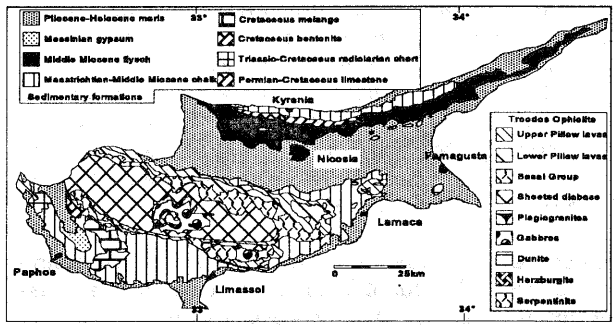

Fig. 1. The Geology of Cyprus

sequence is among one of the best exposed in the world and has been studied in detail by various workers in terms of petrology and mineralogy, tectonic setting, and mineral potential (Greenbaum 1977; Constantinou and Govett 1972; 1973). From the base to the top of the ophiolite sequence, seven major lithologic units can be differentiated. The base of the ultramafic mantle sequence is formed by medium to coarse grained harzburgites containing over 80% olivine and orthopyroxenes (enstatite). The harzburgites gradually grade into dunites composed almost entirely of olivine. The base of the crustal sequence is formed by layered gabbros which at the top of the sequence often are intruded by dykes of granites. The gabbros are overlain by a sheeted dyke complex of closely-packed, nearly vertical doleritic dykes that are often metamorphosed at green-schist facies. Above the sheeted dyke complex is a group of pillow lavas subdivided into a lower pillow lava and a upper pillow lava. The lower pillow lavas contain up to 50% dykes and are of andesitic basalt and quartz andesite. Typically these lavas display plagioclase and pyroxene phenocrysts in a groundmass of altered plagioclase. Albitization and celadonite alteration are common. The upper pillow lavas contain basalt, olivine basalt and ultrabasic

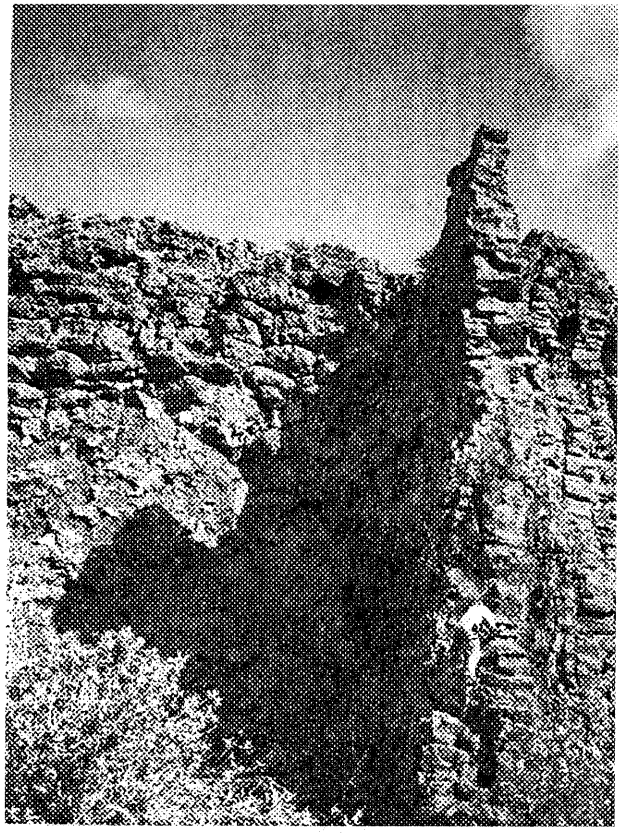

Fig. 2. Pillow lava sequence intruded by dikes

SPECTRAL STRATIGRAPHY

The aim of this section is to establish spectral characteristics that can be used to differentiate the main lithological units that encompass the ore bodies of interest. First we measured and described rock spectra of the different units after which we measured soil spectra. These were measured with the Portable Infrared Mineral Analyzer (PIMA II); a dual field-of-view handheld field spectroradiometer that covers the 1.3 to 2.5μm wavelength region with a 7-10nm spectral resolution and a 2.5nm sampling interval. In thsi paper these spectra will not be discussed at length. The reflectance spectroscopy, however, shows that it is theoretically possible to discriminate the different lithological units based on the soils that develop on them. It should be noted that the outcrops are

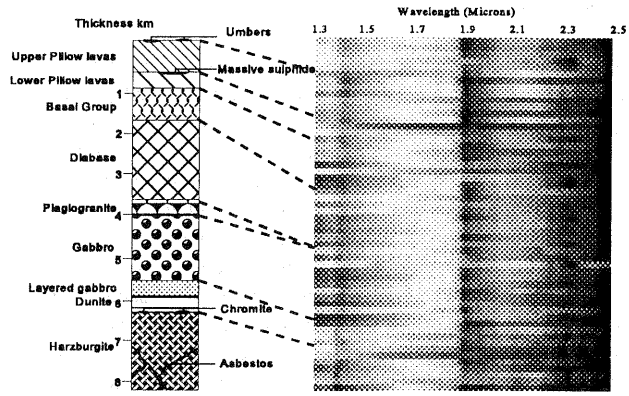

Fig. 3. Stacked spectral sequence through the ophiolites

pillow lavas and a few dykes (Fig. 2). Most pillow lavas contain olivine phenocrysts that are commonly altered to calcite and zeolite-facies minerals. The boundary between the sheeted dyke complex and the lower pillow lavas is formed by a transition zone often referred to as the basal group.

Cyprus was one of the worlds largest producers of asbestos associated with the harzburgites of the Troodos ultramafic sequence. Asbestos occurs in veins within brecciated zones of serpentinized harzburgite, mainly as the hydrated magnesium silicate mineral chrysotile. Near the contact of the harzburgites and dunites, small chromite bodies occur either as isolated pods and layers in the dunite or in the harzburgite within dunite lenses. Typically these ores contain 47% Cr_2O_3 and a Cr/Fe ratio of 2.7 (Greenbaum 1977) after concentration. Massive metallic sulphide deposits are nearly all confined to the contact of the lower and upper pillow lavas (Constantinou and Govett 1973). Pyrites and marcasites are the primary sulphides with minor amounts of chalcopyrites associated with traces of gold and silver. The main secondary minerals formed due to secondary enrichment and leaching are chalcocite, covellite and bornite. These sulphide deposits are thought to have formed near a submarine rift by volcanic exhalative processes which find their modern analogy in the 'black smokers' found near the mid-atlantic ridge. Ochre locally overlies the sulphide ore deposits and are regarded as a sub-aqueous oxidation product of these sulphides. Umbre, defined as a manganese iron rich sediment, is found on top of the upper pillow lavas (Constantinou and Govett 1972).

mostly sparse as is the vegetation cover, thus the major contribution to the image characteristics is thought to come from the soils. Another important aspect is the intermixed nature of the rock types within the units. The different units, however, can be considered mixtures of several rock types. For example the basal group is composed of diabase dykes and andesitic pillow lavas but also dykes occur in the lower pillow lava sequence. A spectral section through the Troodos ophiolite sequence was measured in the field and is shown in Fig. 3 in the form of stacked spectra. In this figure, the dark grey levels indicate low reflectivity whereas the bright areas are high reflectivity. Each line represents one of a total of 54 PIMA spectra through the ophiolite sequence.

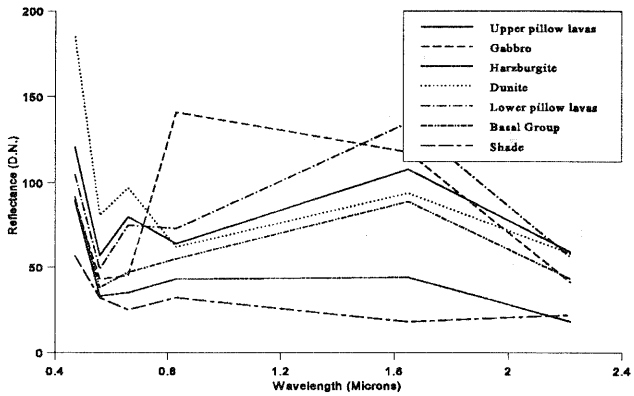

Fig. 4. TM spectra of major geologic units

On basis of field spectroscopic investigations we selected samples and subsequently areas that could serve as spectral end-members for the different lithologies. Their TM spectra as we extracted these from the TM data cube are shown in Fig. 4. It should be noted that non of these end-members can be considered "pure" in the sense that it comprises only one single surface material. On the contrary, we selected those areas that show a representative mix of different ground materials (e.g. green vegetation, dry vegetation, soil, lithology) that are characteristic for the particular lithologic unit.

CROSS CORRELOGRAM SPECTRAL MATCHING (CCSM)

Background

A cross correlogram is constructed by calculating the cross correlation coefficient between a test spectrum, usually a pixel spectrum, and a reference spectrum, usually a laboratory spectrum at different match positions (or lags). By convention, we move the reference spectrum and refer to a negative match position when shifting toward shorter wavelengths and to a positive match position when shifting toward a longer wavelength. Thus match position -1 means that we are calculating the cross correlation between the test spectrum and the reference spectrum in which all channels have been shifted by one channel position number to the lower end of the spectrum. The cross correlation, r_m, at each match position, m, is equivalent to the ordinary linear correlation coefficient and is defined as the product of the covariance and the sum of the standard deviations as

$$r_m = \frac{COV_{t,r}}{s_t s_r} \qquad (1)$$

where $COV_{t,r}$ is the covariance between the overlapped portions of the test spectrum, t, and reference spectrum, r, and s_t and s_r are the corresponding standard deviations. If we denote the test and reference spectrum as λ_t and λ_r, respectively, and define n as the number of overlapping positions, the cross correlation for match position m can be calculated as

$$r_m = \frac{n\Sigma\lambda_r\lambda_t - \Sigma\lambda_r\Sigma\lambda_t}{\sqrt{[n\Sigma\lambda_r^2 - (\Sigma\lambda_r)^2][n\Sigma\lambda_t^2 - (\Sigma\lambda_t)^2]}} \qquad (2)$$

The significance of the cross correlation coefficient can be assessed by the following t-test

$$t = r_m \sqrt{\frac{n-2}{1-r_m^2}} \qquad (3)$$

which has (n-2) degrees of freedom and tests the null hypothesis stating that the correlation between the two spectra at a specific match position is zero.

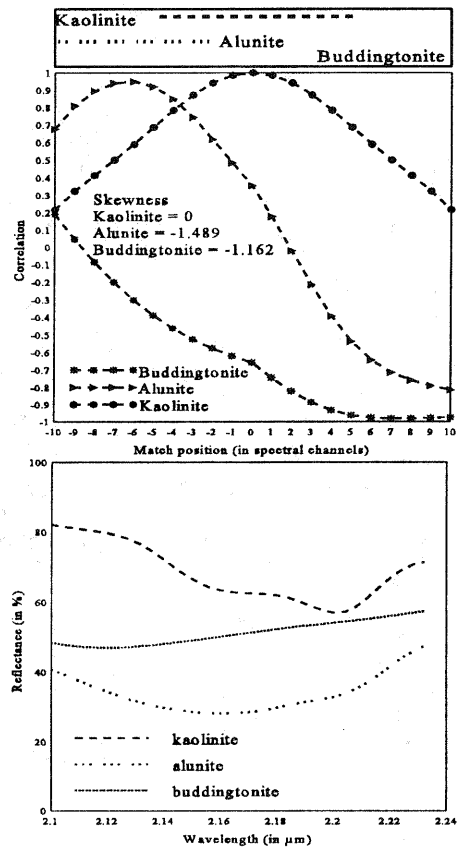

Fig. 5. Cross Correlograms for kaolinite (reference) vs. kaolinite, buddingtonite and alunite (test).

Sensitivity of the method

In order to test the sensitivity of the cross correlogram as a tool for spectral matching, we first applied the method to reflectance spectra from the NASA-JPL laboratory spectral library. Spectra in this library were measured on a Beckman UV 5240 spectrophotometer which has a sampling interval of 1 nm in the wavelength range of 0.4 to 0.8μm, and a sampling interval of 4 nm in the wavelength range of 0.8 to 2.5μm. Bandwidth ranges from 1 nm at 0.4μm to 40 nm at 2.5μm with a spectral resolution (defined as bandwidth/wavelength) better than 2 percent at all wavelengths.

As a reference spectrum we have selected kaolinite and compared it with two other clay minerals; alunite and buddingtonite. Kaolinite has a strong absorption feature at 1.4μm and a double absorption feature centered at 2.16μm and 2.2μm. Due to the lack of H_2O, the feature at 1.9μm is weakly developed or missing. Alunite is characterized by absorption features at 2.16μm and 2.20μm. due to OH frequency stretching and a nearly symmetrical shape in the 2.08-2.28μm. region. A second broad absorption feature occurs at 2.32μm. An absorption feature at 2.02μm. and a vibrational absorption feature due to NH_4 at 2.11μm. are the main diagnostic features distinguishing buddingtonite spectrally from other clay minerals.

The correlogram (not shown here) of kaolinite vs. kaolinite is

symmetric around the match position zero which also has the highest correlation value of one. The symmetry can be expressed in the moment of skewness which we calculate as the correlation at match position ten minus the correlation at match position minus ten. To demonstrate that the cross correlogram is insensitive to differences in albedo, a test spectrum was offset by 10% reflectance which had no effect on the correlogram.The effect of noise on the correlogram is demonstrated by adding a component of 5% random noise to the test spectrum which does not affect the shape characteristics of the correlogram, but results in a decrease of the cross correlation values by 5%. In Fig. 5, the cross correlogram is shown for the spectral matching of kaolinite (as reference spectrum) versus buddingtonite, alunite and kaolinite (as test spectrum). This figure shows the spectra of the minerals in the bottom part of the figure and the cross correlograms in the top part. 3. The function for buddingtonite is highly skewed with the negative moment of skewness indicating that the peak of the correlation coefficients is found when shifting the kaolinite spectrum toward shorter wavelengths. Note that the correlation coefficients were found insignificant for all match positions. The cross correlogram for alunite versus kaolinite shows a peak at match position minus six which corresponds to a shift of the kaolinite reference spectrum of 24 nm toward shorter wavelength.

In summary, the cross correlogram is insensitive to gain factors and random noise affects the values of the correlation coefficients equally at each match position without affecting the shape of the correlogram. The position of the correlation peak in the correlogram is directly related to the relative position of the spectral absorption features that are being compared and the *t*-test provides a means of testing the significance of the correlation coefficients found. Finally, the cross correlogram provides a statistically meaningful comparison between test and reference spectra that can lead to automated mineral mapping from TM data or ultimately as we are now conducting for imaging spectrometer data.

Application of CCSM to TM data from Cyprus

In order to be able to directly compare the ground reflectance measurements with the image data, we attempted to convert the grey level information of the Landsat TM data to physical reflectance values using the ATCOR2 software developed by Richter (1990). This algorithm uses a catalog of atmospheric correction functions that describe a wide range of different conditions in terms of altitude pressure profiles, aerosol type, ground elevation, solar zenith angle, visibility, etc. The program allows to select a atmosphere model for the entire (or parts) of the scene and reference targets with known reflectance properties. The user may also define pixels containing haze or clouds which are treated separately in the correction process. We found problems in selecting a reference spectrum for the scene. On the top of the Troodos massif, dense vegetation is abundant and the vegetation index calculated suggested that in time not much change had occurred. Therefore our field measurements of the target area seemed to yield satisfactory data for the correction. However, we found that the differences in altitudes created an obstacle in image correction. The area of investigation, the Troodos massif, ranges from 150 m. at the low-lying Mesaoria plain to 1920 m. at the highest peak; Mount Olympus. An attempt was made to divide the investigated portion of the scene into sub-areas which were treated individually. This, however, failed because of the lack of reference targets (e.g. dense vegetation or water) in most of the area. On basis of this we decided to work with the raw rather than with the atmospherically corrected TM data. In future with the advent of ATCOR3 (e.g. the atmosphere correction software that incorporates a digital terrain model), which will be available soon (pers. comm. R. Richter, 1995) we hope to be able to directly link field and image spectra.

Fig. 6a. Correlation image for dunites

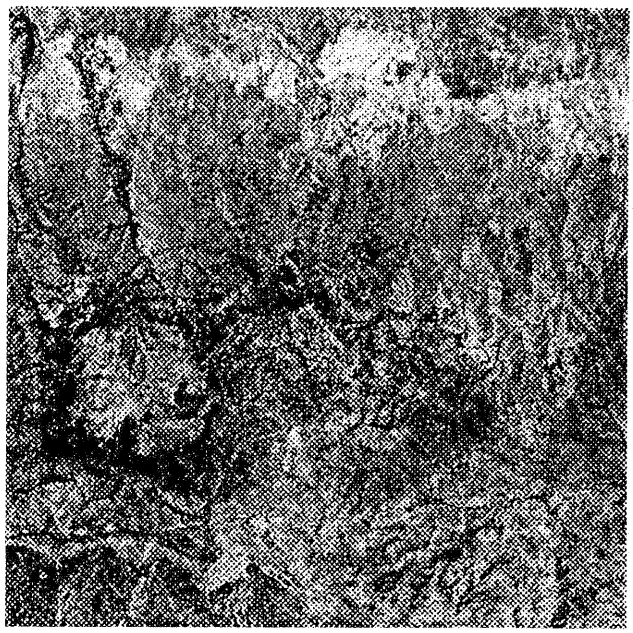

Fig. 6b. Correlation image for the upper pillow lavas

CCSM may yield three parameters that can serve to map surface mineralogy from broad-band image data and ultimately from hyperspectral image data: the cross correlation at match position zero, the significance of this correlation and the moment of skewness of the correlogram. Here we use only the first indicator. In Fig. 6, examples of cross correlation images are given. These are

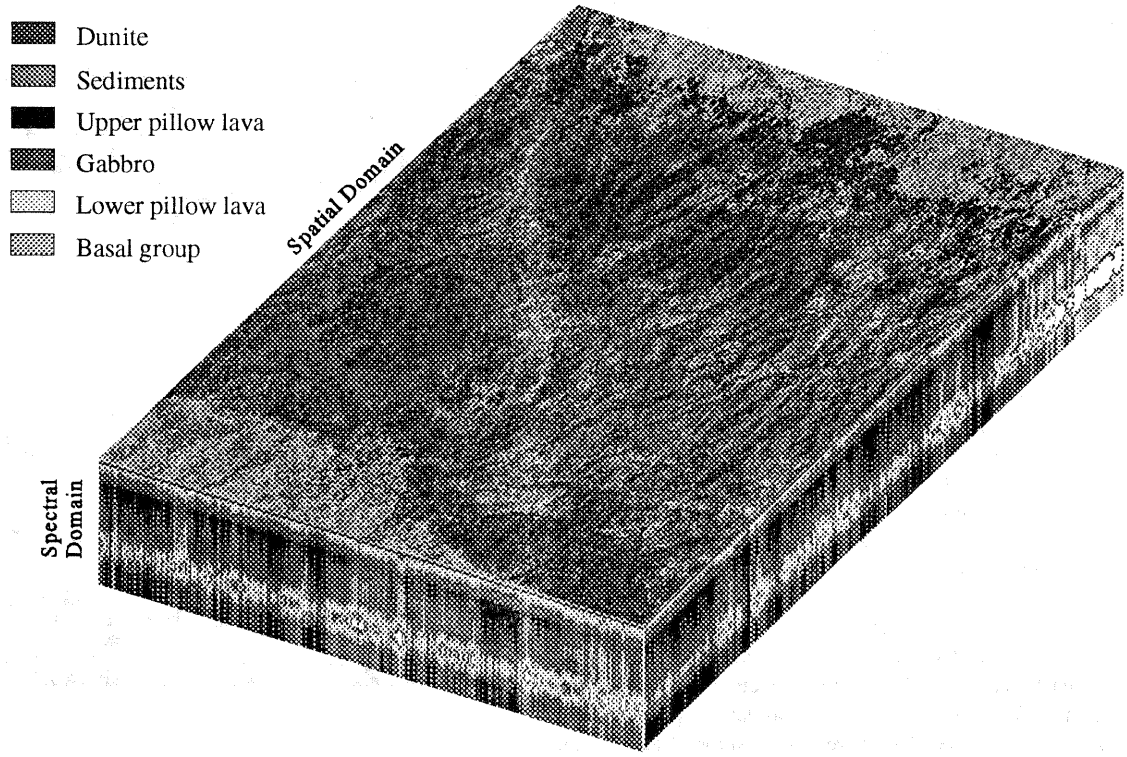

Fig. 7. Final CCSM representation (original is in color).

displayed in grey scale with white corresponding to the highest positive correlation.

Our final interpretation shown in Fig. 7 is based on the CCSM results. For each CCSM image we extracted the pixels that most closely matched the input spectrum (e.g. those with correlation values within 10% of the perfect value). These were color-coded, combined with the pixels from the other CCSM images and overlain for display purposes onto TM band 5. In case one pixel was assigned to two units, we disregarded it. Fig. 7 shows a three-dimensional spectral and spatial TM data cube displaying our results. The spectral domain shows a color-coded stacked slice constructed using the six Landsat TM bands displayed from the top (TM 1) to the bottom (TM 7). Color-coding is done according to reflectance relative to average; red and yellow are high reflectance and purple and black are low reflectance. The spatial domain shows the key lithologies. Note that copper mineralization is known to occur along the boundary of upper and lower pillow lava series. Especially the upper pillow lava series is very well marked in our final image.

CONCLUSIONS

Detailed geologic mapping and mineral prospecting has been carried out over the last decades in Cyprus, thus the present study is of a purely scientific nature. However it demonstrates the potential of using advanced image processing techniques for mineral prospecting in ultramafic terrains. We were able to locate the boundary between two lava sequences which forms an important target for copper exploration. Furthermore, serpentinized dunites were mapped that may host asbestos deposits. At a reconnaissance level, CCSM may contribute to a first assessment of mineral potential in ultramafic terrains although it will not replace traditional geologic field practice.

ACKNOWLEDGEMENTS

We would like to thank Dr. G. Constantinou, Dr. A Charalambides, and Dr. C. Xenophontos of the Geological Survey of Cyprus for their help in organising and conducting the necessary field work.

REFERENCES

CONSTANTINOU, G., and GOVETT, G.J.S., 1972, Genesis of sulphide deposits, ochre and umber of Cyprus. *Transactions of the Institute of Mining and Metallurgy*, **81**, pp. 34-46.

CONSTANTINOU, G., and GOVETT, G.J.S., 1973, Geology, Geochemistry, and Genesis of Cyprus Sulphide deposits. *Economic Geology*, **68**, pp. 843-858.

DAVIDSON, D., BRUCE, B. and JONES, D., 1993, Operational remote sensing mineral exploration in semi-arid environment: the Troodos massif, Cyprus. In *Proceedings of the*

Ninth Thematic Conference on Geologic Remote Sensing, ERIM held in Pasadena, California, U.S.A., on 8-11 February, 1993, pp. 845-859.

GREENBAUM, D., 1977, The Chromitiferous rocks of the Troodos Ophiolite Complex, Cyprus. *Economic Geology*, **72**, pp. 1175-1194.

RICHTER, R., 1990, A fast atmospheric correction algorithm applied to Landsat TM images. *International Journal of Remote Sensing*, **11**, pp. 159-166.